Nuclear Inst. and Methods in Physics Research B 443 (2019) 1–4

Contents lists available at ScienceDirect

Nuclear Inst. and Methods in Physics Research B

journal homepage: www.elsevier.com/locate/nimb

Natural nickel as a proton beam energy monitor for energies ranging from 15 to 30 MeV

Tara Mastren[a,b], Christiaan Vermeulen[a], Mark Brugh[a], Eva R. Birnbaum[a], Meiring F. Nortier[a], Michael E. Fassbender[a,*]

[a] Chemistry Division, Los Alamos National Laboratory, P.O. Box 1663, Los Alamos, NM 87545, USA
[b] Nuclear Engineering Program, Department of Civil and Environmental Engineering, University of Utah, 110 Central Campus Drive, Suite 2000b, Salt Lake City, UT 84112, USA

ARTICLE INFO

Keywords:
Proton beam
Beam energy
Monitor reactions
Ni-57
Co-57

ABSTRACT

The degradation of proton beam energy within a target stack was monitored via product nuclide ratios at the Los Alamos Isotope Production Facility (LANL-IPF). Nuclear reaction channels employed as energy monitors included ^{Nat}Ni(p,x)^{57}Co and ^{Nat}Ni(p,x)^{57}Ni. Natural nickel foils (thicknesses 0.025 mm) were used to determine proton beam energies ranging from 15 to 30 MeV. Energy values were estimated from a fitted ^{57}Ni/^{57}Co production activity ratio curve, which, in turn, was calculated from formation cross section data. Isotope production yields in the low energy "C" slot at LANL-IPF are very sensitive to beam energy, and differences of several MeV can translate into a drastic effect on overall production yields and radiochemical purity. Proton energies determined in this target stack position using nickel foils will serve as a basis to optimize radionuclide production in terms of product yield maximization and by-product minimization.

1. Introduction

Monitoring the energy of protons incident on targets is an important technique for the optimization of radionuclide production [1–5]. Knowledge of the incident energy aids in designing targets of optimal thickness that allow the highest product nuclide yield with the least amount of undesired by-products. This is especially true in the case of multi-target stacks such as those employed at the Isotope Production Facility (IPF) at Los Alamos National Laboratory (LANL). In these cases, the beam is degraded as it passes through each target, complicating energy measurement and prediction. Currently, copper foils are often used for monitoring low proton energies (< 30 MeV) [6–9]. In this case, however, energy analyses rely on the activity ratios of short-lived zinc isotopes: ^{62}Zn (9.22 h)/^{63}Zn (38.5 m) and ^{62}Zn (9.22 h)/^{65}Zn (243.9 d). This requires that monitor foils be subjected to γ-ray analysis quickly, i.e., within hours to days of the irradiation.

At IPF quick γ-ray analysis is not always possible due to shipping logistics, since target materials from IPF have to be shipped to the count room facility, located in a separate building, via public roads. This shipping process can take days due to required approvals and shipping schedules. Therefore, a method of monitoring beam energy utilizing radionuclides with half-lives greater than one day is advantageous. The most common way to measure beam energy with a monitor foil is through the evaluation of the energy and time dependent activity ratio of two co-produced radionuclides, which we will call A and B. Prerequisites for such an analysis are (1) that nuclides *A* and *B* are both formed in the applicable energy range, and (2) well-measured excitation functions $\sigma_A(E)$ and $\sigma_B(E)$, for which the ratio function $r = \sigma_A(E)/\sigma_B(E)$ is strictly monotonic (either increasing or decreasing) within the applicable energy range. If both conditions are met, the ratios of measured nuclide activities, as projected back in time to end-of-bombardment (EOB), will directly correspond to the effective energy of the proton beam that traversed through the target stack.

Isotope production is routinely performed at IPF with an incident proton beam energy of 100 MeV ± (0.1 MeV). In a typical production target stack (Fig. 1), the targets occupy slots labelled "**A**", "**B**" and "**C**" which represent the high, medium, and low energy positions respectively. While penetrating upstream targets, the proton beam loses energy ("degrades"), so that the energy of protons incident on downstream targets progressively decreases, and the extent of energy degradation depends on material and thickness of the upstream targets. The C-slot position is normally suitable for lower energy reactions (< 40 MeV incident energy). C-slot isotope production is of interest for several research applications including ^{230}U, ^{44}Ti, ^{119}Te, and ^{186}Re

* Corresponding author.
E-mail addresses: mifa@lanl.gov, radiochemistry@outlook.com (M.E. Fassbender).

https://doi.org/10.1016/j.nimb.2019.01.038
Received 20 December 2018; Received in revised form 18 January 2019; Accepted 23 January 2019

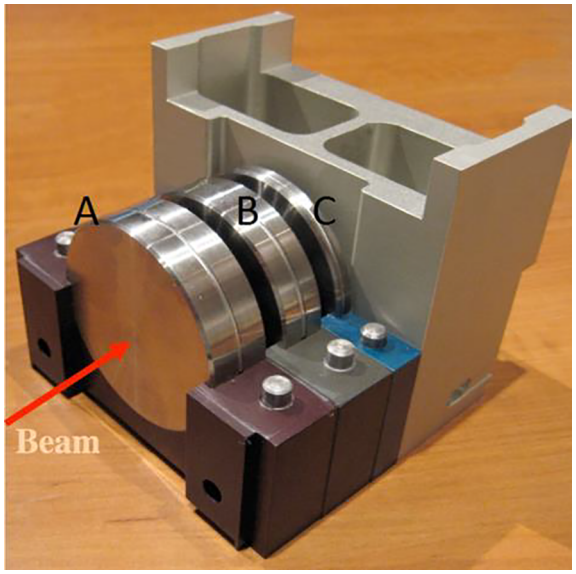

Fig. 1. A typical LANL-IPF production stack showing targets occupying "**A**", "**B**", and "**C**" slots.

Table 1
Characteristic gamma rays of radionuclides monitored for energy determination.

Radionuclide	Characteristic Gamma Energy (keV)	Percent Abundance
^{57}Ni	1377.6	81.7
	127.2	16.7
^{57}Co	122.1	85.6
	136.5	10.7

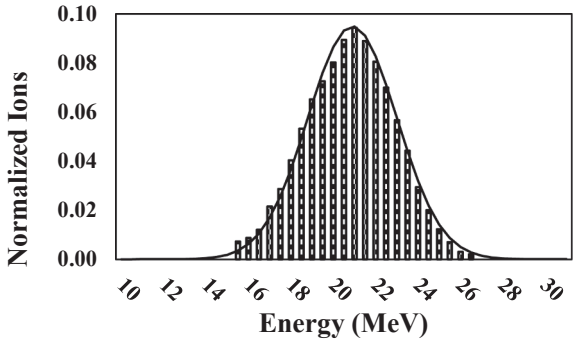

Fig. 2. Gaussian fit of the proton energy distribution after degradation to 24 MeV from 100 MeV with aluminum degraders. FWHM was determined to be 5.1 MeV.

[10,11]. In the case of ^{186}Re, the incident energy is very important and deviations can result in significant reductions in production yields [12]. However, accurate knowledge of the energy of protons entering the C-slot is nontrivial owing to both beam straggle, uncertainties in physical target thickness, the in-beam density of the targets, and aggregate error propagation in the energy degradation formalism that describes the beam energy loss in materials according to classical electrodynamics. This sometimes leads to significant discrepancies between the predicted and actual C-slot incident energy.

Nickel foils of natural isotopic composition were used in our study. Nickel has previously been utilized in monitoring nuclear reactions [2,5,7]. Proton induced reactions on nickel foils have been extensively studied, and excitation functions of these reactions are well characterized [9,13–16]. For proton energies between 15 and 30 MeV, the formation of ^{57}Ni (35.6 h) and ^{57}Co (271.8 d) meets the above requirements for monitor reactions.

Herein, we report the use of the end-of-bombardment (EOB) ^{57}Ni/^{57}Co activity ratio for the monitoring of IPF "C-Slot" energies.

2. Materials and methods

2.1. Energy distribution of the proton beam in the nickel foil body

A Stopping Power Range of Ions in Matter (SRIM) simulation was performed that simulated 100 MeV protons penetrating an aluminum degrader sufficiently thick to degrade the median proton energy to 24 MeV in order to obtain a Gaussian energy distribution of the proton beam. Ten thousand transmitted ions were binned at 0.5 MeV intervals. The population of each bin was normalized to a sum of one (over all bins) and plotted vs energy and fit with a Gaussian normal distribution as described in Eq. (1) where A is the amplitude, μ is the centroid energy, E is the proton energy and σ is the standard deviation.

$$Ratio\ of\ Ions = A * e^{\frac{-(E-\mu)^2}{2\sigma^2}} \quad (1)$$

2.2. Evaluation of ^{Nat}Ni(p,x)^{57}Ni and ^{Nat}Ni(p,x)^{57}Co cross section data

Experimental cross section data for the proton induced reactions ^{nat}Ni(p,x)^{57}Ni [9,13–15] and ^{nat}Ni(p,x)^{57}Co [13,14,16] were obtained from the Experimental Nuclear Reaction Database Version of 2018–04-25 (EXFOR) [17] https://www-nds.iaea.org/exfor/exfor.htm. Cross section data selected for the production of ^{57}Co was for its cumulative formation. Cross section data for proton energies ranging from 13 to 40 MeV was plotted vs energy and fit with a sixth order polynomial. Fits were used to obtain smoothed excitation functions for proton energies ranging from 15 to 30 MeV.

2.3. ^{57}Ni/^{57}Co activity ratios vs energy calculations

The ratio of the expected ^{57}Ni/^{57}Co activity was calculated using Eq. (2) where A_i is activity of nuclide i, σ_i is the effective cross section, λ_i is the decay constant, and t_b is the bombardment time with $i = 1, 2$ representing ^{57}Ni and ^{57}Co respectively. Effective cross sections for each radionuclide at a given energy were obtained assuming a Gaussian distribution of the energy around the average given energy, as described in Section 2.1, to more accurately represent the experimental conditions at LANL IPF. Assuming the average energy is the centroid of the Gaussian, the normalized distribution of the energy at 5 MeV to the left and right of the median energy was taken into account when determining the effective cross section at a given energy.

$$\frac{A_1}{A_2} = \frac{\sigma_1\left(1 - e^{-\lambda_1 t_b}\right)}{\sigma_2\left(1 - e^{-\lambda_2 t_b}\right)} \quad (2)$$

2.4. Proton energy measurements with Natural nickel foils

Four nickel foils (thicknesses 0.025 mm, tolerance < 0.010 mm, 99.999% purity from Goodfellow USA, Coraopolis, PA) were irradiated with protons (20 μA average current; 30 min duration) in the 15–30 MeV energy range degrading the incoming 100 MeV proton beam with aluminum degraders occupying slots "**A**" and "**B**" (comp Fig. 1). The foils were shipped to the hot cell facility and dissolved in 10 M HNO_3. The dissolved nickel foil was brought to dryness, re-dissolved in 5 mL 10 M HNO_3, and placed into a pre-weighed 20 mL scintillation vial. The weight of the nickel solution was then determined and dilutions were made by weight to represent dilutions of approximately 1:5, 1:10, and 1:20. The ^{57}Ni and ^{57}Co activities were then determined via High Purity Germanium Spectroscopy (HPGe) using the characteristic gamma rays shown in Table 1. The activities of ^{57}Ni and

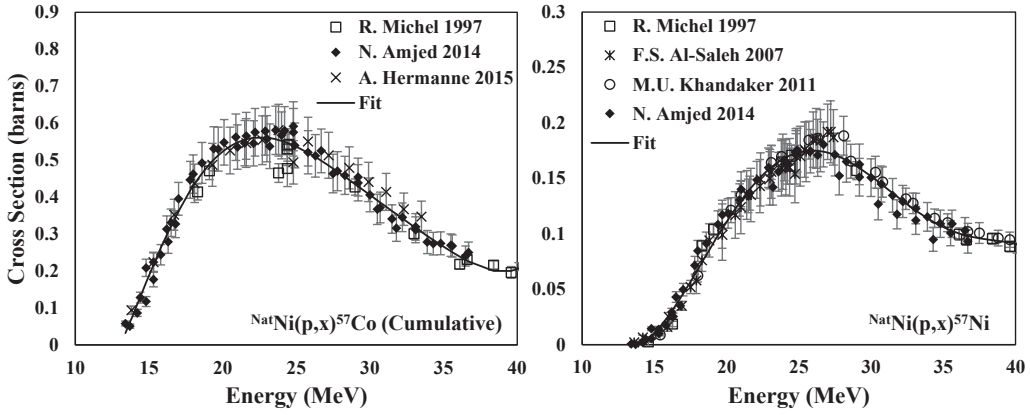

Fig. 3. Excitation functions and fit for the reactions ^{Nat}Ni(p,x)^{57}Ni and ^{Nat}Ni(p,x)^{57}Co (cumulative).

Table 2
Calculated cross sections for the ^{Nat}Ni(p,x)^{57}Ni and ^{Nat}Ni(p,x)^{57}Co (cumulative) reactions for proton energies ranging from 15 to 30 MeV.

Energy (MeV)	^{Nat}Ni(p,x)^{57}Ni (mb)	^{Nat}Ni(p,x)^{57}Co (mb)
15	10	188
15.5	18	235
16	26	280
16.5	36	322
17	46	362
17.5	57	398
18	68	430
18.5	79	459
19	90	484
19.5	100	505
20	111	523
20.5	121	537
21	130	548
21.5	138	555
22	146	560
22.5	153	561
23	159	560
23.5	164	557
24	168	552
24.5	171	545
25	174	536
25.5	175	526
26	175	515
26.5	175	503
27	173	490
27.5	171	477
28	168	463
28.5	165	449
29	161	435
29.5	157	420
30	152	406

^{57}Co were corrected to end of bombardment (EOB), and ^{57}Co cumulative EOB yields were calculated by correcting for the contribution from the decay of ^{57}Ni. Decay during bombardment was taken into account for both isotopes measured.

2.5. High purity germanium (HPGe) spectrometry

Gamma-ray spectrometry was conducted using an EG & G Ortec Model GMX-35200-S HPGe detector system in combination with a Canberra Model 35-Plus multichannel analyzer. Detector diameter was 50.0 mm; detector length 53.5 mm; Be window thickness 0.5 mm; outer dead-layer thickness 0.3 μm. Detector response function determination and evaluation were performed using standards of radionuclide mixtures containing ^{241}Am, ^{109}Cd, ^{57}Co, ^{139}Ce, ^{203}Hg, ^{113}Sn, ^{137}Cs, ^{88}Y, ^{60}Co, traceable to the National Institute of Standards and Technology (NIST) and supplied by Eckert & Ziegler, Atlanta, GA, USA. Relative total source activity uncertainties ranged from 2.6% to 3.3%. Counting dead time was kept below 10%.

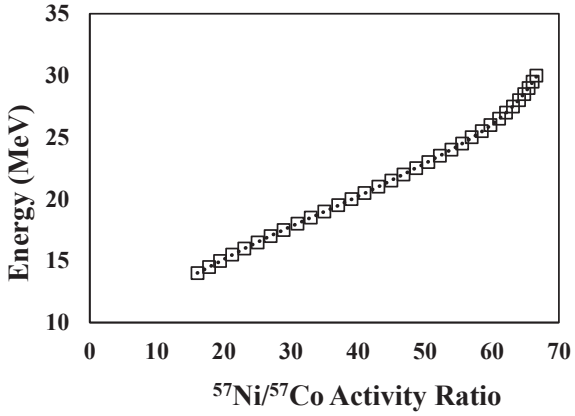

Fig. 4. Energy vs ^{57}Ni/^{57}Co activity ratio.

3. Results and discussion

3.1. Energy distribution of the proton beam in the nickel foil body

The normalized and binned distribution of the proton energy was fit with a Gaussian function and is shown in Fig. 2. The Full Width Half Max (FWHM, ~2.34σ) was found to be 5.1 MeV.

3.2. Evaluation of ^{Nat}Ni(p,x)^{57}Ni and ^{Nat}Ni(p,x)^{57}Co cross section data

Excitation functions for the proton induced formation of ^{57}Ni and ^{57}Co in nickel targets are shown in Fig. 3. The data was fit with a sixth order polynomial and is shown as solid lines in Fig. 3. Interpolated cross sections for each isotope for energies ranging from 15 to 30 MeV are shown in Table 2.

3.3. ^{57}Ni/^{57}Co activity ratios vs energy calculations

Effective cross section values for ^{57}Ni and ^{57}Co were calculated using the interpolated cross sections in Table 2 taking into account the energy distribution of the proton beam. Energy vs ^{57}Ni/^{57}Co (cumulative) activity ratios were then calculated, graphed and fit with a 6th-order polynomial (Fig. 4).

Table 3
Energy determinations of 100 MeV proton beam degraded to values < 30 MeV with an aluminum degrader.

Date of Irradiation	Measured Energy (MeV)	Predicted Energy (MeV) [18]	^{57}Co Yield (% of Theoretical)	^{57}Ni Yield (% of Theoretical)
January 2017	19 ± 1	23.5	100	100
August 2017	27 ± 1	29.3	90	89
September 2017	24 ± 1	29.3	89	90
January 2018	27 ± 1	29.3	90	90

3.4. Proton energy measurements with Natural nickel foils

The energy of the beam was measured four times with a nickel foil and the results are shown in Table 3. The error in the energy measurement was determined by least squares regression of the fit of the cross-sections and activity ratios. Proton energies ranged from 19 to 27 MeV. Production yields of ^{57}Ni and ^{57}Co were compared to theoretical yields based on the measured energy and found to fall within 10% error. The measured median energies were in disagreement with predicted median energies based upon Anderson and Ziegler [18].

This method was used to aid in increasing the production yield of ^{119m}Te. The incident beam energy was adjusted for the difference in measured vs predicted energies; increasing the yield of ^{119m}Te 1000 fold providing a corresponding data point to the usefulness of this method. The discrepancy between the measured and predicted median energies is not yet well understood, but possible contributions could be from the uncertainty in the multiple degrading layers in the Isotope Production Facility configuration. To help characterize this uncertainty, we plan to perform a comprehensive study of the effect of the density gradient in the first targets on the downstream energy distribution. This will be achieved by using the current technique while pixelating the target foil using a collimated XY scanning system.

4. Conclusions

Natural nickel foils were used successfully to measure the energy of degraded proton beams between 15 and 30 MeV. Isotope production yields in the low energy “C Slot” at LANL-IPF are very sensitive to beam energy, and differences of several MeV can propagate into a drastic effect on overall production yields. In a recent experiment, the production yield of ^{119m}Te was found to be extremely low, indicating an energy window mismatch in the target stack. Using the current method to determine and adjust the input energy for the target, the yield of ^{119m}Te could be increased 1000 fold showing correct capture of the optimal energy window. This method has already helped to optimize conditions at the IPF so that the highest possible yields can be obtained in the difficult to predict, lower energy irradiation positions. In future C-slot irradiations, this reaction will be utilized to ensure that the incident beam energy is within the desired range for the optimal production of the desired radionuclide.

Acknowledgements

We gratefully recognize the United States Department of Energy, Office of Science, Isotope Development and Production for Research and Applications subprogram within the Office of Nuclear Physics, Grant FOA LAB 14-1099.

References

[1] P. Kopecky, F. Szelecsenyi, T. Molnar, P. Mikecz, F. Tarkanyi, Excitation-Functions of (P, Xn) reactions on (Nat)Ti – monitoring of bombarding proton-beams, Appl. Radiat. Isot. 44 (1993) 687–692.
[2] F. Tarkanyi, F. Szelecsenyi, P. Kopecky, Excitation-functions of proton-induced nuclear-reactions on natural nickel for monitoring beam energy and intensity, Appl. Radiat. Isot. 42 (1991) 513–517.
[3] J.B. Cumming, Monitor reactions for high energy proton beams, Ann. Rev. Nucl. Sci. 13 (1963) 261–286.
[4] S. Takacs, F. Tarkanyi, M. Sonck, A. Hermanne, Investigation of the Mo-nat(p, x)Tc-96mg nuclear reaction to monitor proton beams: new measurements and consequences on the earlier reported data, Nucl. Instrum. Meth. B 198 (2002) 183–196.
[5] A. Hermanne, A.V. Ignatyuk, R. Capote, B.V. Carlson, J.W. Engle, M.A. Kellett, T. Kibedi, G. Kim, F.G. Kondev, M. Hussain, O. Lebeda, A. Luca, Y. Nagai, H. Naik, A.L. Nichols, F.M. Nortier, S.V. Suryanarayana, S. Takacs, F.T. Tarkanyi, M. Verpelli, Reference cross sections for charged-particle monitor reactions, Nucl. Data Sheets 148 (2018) 338–382.
[6] P. Kopecky, Proton-beam monitoring via the Cu(P, X) Co-58, Cu-63 (P, 2n) Zn-62 and Cu-65 (P, N) Zn-65 reactions in copper, Int. J. Appl. Radiat. Isot. 36 (1985) 657–661.
[7] S. Takacs, F. Tarkanyi, M. Sonck, A. Hermanne, New cross-sections and intercomparison of proton monitor reactions on Ti Ni and Cu, Nucl. Instrum. Meth. B 188 (2002) 106–111.
[8] K. Gagnon, F. Benard, M. Kovacs, T.J. Ruth, P. Schaffer, J.S. Wilson, S.A. McQuarrie, Cyclotron production of (99m)Tc: experimental measurement of the (100)Mo(p, x)(99)Mo, (99m)Tc and (99g)Tc excitation functions from 8 to 18 MeV, Nucl. Med. Biol. 38 (2011) 907–916.
[9] F.S. Al Saleh, K.S. Al Mugren, A. Azzam, Excitation functions of (p, x) reactions on natural nickel between proton energies of 2.7 and 27.5 MeV, Appl. Radiat. Isot. 65 (2007) 104–113.
[10] T. Mastren, V. Radchenko, H.T. Bach, E.R. Balkin, E.R. Birnbaum, M. Brugh, J.W. Engle, M.D. Gott, J. Guthrie, H.M. Hennkens, K.D. John, A.R. Ketring, M. Kuchuk, J.R. Maassen, C.M. Naranjo, F.M. Nortier, T.E. Phelps, S.S. Jurisson, D.S. Wilbur, M.E. Fassbender, Bulk production and evaluation of high specific activity (186)gRe for cancer therapy using enriched (WO3)-W-186 targets in a proton beam, Nucl. Med. Biol. 49 (2017) 24–29.
[11] V. Radchenko, J.W. Engle, D.G. Medvedev, J.M. Maassen, C.M. Naranjo, G.A. Unc, C.A.L. Meyer, T. Mastren, M. Brugh, L. Mausner, C.S. Cutler, E.R. Birnbaum, K.D. John, F.M. Nortier, M.E. Fassbender, Proton-induced production and radiochemical isolation of Ti-44 from scandium metal targets for Ti-44/Sc-44 generator development, Nucl. Med. Biol. 50 (2017) 25–32.
[12] M.E. Fassbender, B. Ballard, E.R. Birnbaum, J.W. Engle, K.D. John, J.R. Maassen, F.M. Nortier, J.W. Lenz, C.S. Cutler, A.R. Ketring, S.S. Jurisson, D.S. Wilbur, Proton irradiation parameters and chemical separation procedure for the bulk production of high-specific-activity Re-186g using WO3 targets, Radiochim. Acta 101 (2013) 339–346.
[13] R. Michel, R. Bodemann, H. Busemann, R. Daunke, M. Gloris, H.J. Lange, B. Klug, A. Krins, I. Leya, M. Lupke, S. Neumann, H. Reinhardt, M. SchnatzButtgen, U. Herpers, T. Schiekel, F. Sudbrock, B. Holmqvist, H. Conde, P. Malmborg, M. Suter, B. DittrichHannen, P.W. Kubik, H.A. Synal, D. Filges, Cross sections for the production of residual nuclides by low- and medium-energy protons from the target elements C, N, O, Mg, Al, Si, Ca, Ti, V, Mn, Fe Co, Ni, Cu, Sr, Y, Zr, Nb, Ba and Au, Nucl. Instrum. Meth. B 129 (1997) 153–193.
[14] N. Amjed, F. Tarkanyi, A. Hermanne, F. Ditroi, S. Takacs, M. Hussain, Activation cross-sections of proton induced reactions on natural Ni up to 65 MeV, Appl. Radiat. Isot. 92 (2014) 73–84.
[15] M.U. Khandaker, K. Kim, M. Lee, K.S. Kim, G. Kim, Excitation functions of (p, x) reactions on natural nickel up to 40 MeV, Nucl. Instrum. Meth. B 269 (2011) 1140–1149.
[16] A. Hermanne, R.A. Rebeles, F. Tarkanyi, S. Takacs, Excitation functions of proton induced reactions on Os-nat up to 65 MeV: Experiments and comparison with results from theoretical codes, Nucl. Instrum. Meth. B 345 (2015) 58–68.
[17] National Nuclear Data Center, Experimental Nuclear Reaction Database, Brookhaven National Laboratory, 1994.
[18] H.H. Andersen, J.F. Ziegler, Hydrogen Stopping Powers and Ranges in All Elements, P. Press, 1977.